NPL REPORT DEPC-MPE 001

VAMAS TWA 22 Mechanical Property Measurement of Thin Films and Coatings

A ROUND ROBIN TO MEASURE THE ADHESION OF THIN COATINGS

G Aldrich-Smith[1], N.M. Jennett[1] & J Housden[2]

[1] Materials Performance
National Physical Laboratory. UK.

[2] Tecvac Ltd, Cambridge, UK.

September 2004

VAMAS TWA 22
Mechanical Property Measurement of Thin Films and Coatings

A ROUND ROBIN TO MEASURE THE ADHESION OF THIN COATINGS

G Aldrich-Smith[1] & N.M. Jennett[1]

Materials Performance,
Engineering and Process Control Division,
National Physical Laboratory.

J Housden[2]
Tecvac Ltd, Cambridge UK.

EXECUTIVE SUMMARY

An interlaboratory exercise on 5μm thick chromium nitride (CrN) coated AISI 304 austenitic stainless steel coupons was undertaken to evaluate and compare test methods for adhesion of thin coatings. Test coupons were deposited with and without thin (25nm & 50nm) gold-palladium interlayers. These interlayers were designed to vary the effective adhesion of the CrN in a controlled way without significantly altering the CrN coating fracture properties. The interlaboratory exercise was conducted by an international group of laboratories examining Rockwell indentation, scratch testing, uniaxial tensile and four-point bend. None of the tests were able to discriminate between coupons with or without the interlayer. The new EU Community Bureau of Reference scratch test reference material (BCR-692), distributed to participants to assist in the calibration of scratch test instruments used in this study, was shown to be able to diagnose instrument problems.

ISSN 1744-0262

National Physical Laboratory
Teddington, Middlesex, UK, TW11 0LW

We gratefully acknowledge the financial support of the UK Department of
Trade and Industry (National Measurement System Policy Unit)

Approved on behalf of Managing Director,
NPL, by Dr C Lea, Knowledge Leader (Division),
Engineering and Process Control Division

VAMAS

Technical Working Area 22
Mechanical Property Measurement of Thin Films and Coatings

A ROUND ROBIN TO MEASURE THE ADHESION OF THIN COATINGS

Report No. 46
ISSN 1016-2186
July 2004

The Versailles Project on Advanced Materials and Standards supports trade in high technology products through international collaborative projects aimed at providing the technical basis for drafting codes of practice and specifications for advanced materials. The scope of the collaboration embraces all agreed aspects of enabling science and technology - databases, test methods, design standards, and materials technology - which are required as a precursor to the drafting of standards for advanced materials. VAMAS activity emphasizes collaboration on pre-standards measurement research, intercomparison of test results, and consolidation of existing views on priorities for standardization action. Through this activity, VAMAS fosters the development of internationally acceptable standards for advanced materials by the various existing standards development organizations.

VAMAS

Technical Working Area 22
Mechanical Property Measurement of Thin Films and Coatings

A ROUND ROBIN TO MEASURE THE ADHESION OF THIN COATINGS

Giles Aldrich-Smith[1], Nigel Jennett[1] & Jonathan Housden[2].

[1] Materials Centre, National Physical Laboratory, Teddington, Middlesex, U.K.
[2] Tecvac Ltd, Buckinway Business Park, Swavesey, Cambridge, CB4 5UG, U.K.

e-mail: giles.aldrich-smith@npl.co.uk

Report No. 46
ISSN 1016-2186
July 2004

Contents

1. INTRODUCTION. 8

2. EXPERIMENTAL. 9
2.1. SCOPING STUDY. 9
2.2. INTERLABORATORY EXERCISE TEST COUPONS. 10
2.2.1 DEPOSITION. 10
2.2.2. CHARACTERISATION. 11
2.3. INTERLABORATORY TESTS. 12

3. RESULTS AND DISCUSSION. 13
3.1. DEPOSITION AND CHARACTERISATION. 13
3.2. ROCKWELL INDENTATION. 14
3.3. SCRATCH TESTING. 14
3.4. TENSILE AND FOUR-POINT BEND TESTING. 18
3.5. THERMAL TESTING. 19

4. CONCLUSIONS. 19

5. REFERENCES. 20

ACKNOWLEDGMENTS. 21

ANNEXE Independent evaluation of toughness: Interface and film 22

A ROUND ROBIN TO MEASURE THE ADHESION OF THIN COATINGS

Giles Aldrich-Smith & Nigel Jennett
NPL, U.K

Jonathan Housden
Tecvac Ltd, U.K.

Abstract

An interlaboratory exercise on 5µm thick chromium nitride (CrN) coated AISI 304 austenitic stainless steel coupons was undertaken to evaluate and compare test methods for adhesion of thin coatings. Test coupons were deposited with and without thin (25nm & 50nm) gold-palladium interlayers. These interlayers were designed to vary the effective adhesion of the CrN in a controlled way without significantly altering the CrN coating fracture properties. The interlaboratory exercise was conducted by an international group of laboratories examining Rockwell indentation, scratch testing, uniaxial tensile and four-point bend. None of the tests were able to discriminate between coupons with or without the interlayer. The new EU Community Bureau of Reference scratch test reference material (BCR-692), distributed to participants to assist in the calibration of scratch test instruments used in this study, was shown to be able to diagnose instrument problems.

1. INTRODUCTION.

VAMAS (Versailles Project on Advanced Materials and Standards) technical work area 22 was set up to co-ordinate international efforts in the development of standards for measuring the mechanical properties of thin films and coatings. This was in response to the growing take-up and economic importance of Surface Engineering in a wide range of industries and the lack of quantitative methodologies to generate mechanical properties for thin (<10μm) films. Coatings technology is fundamentally dependent upon good adhesion between the coating and the substrate, and in many cases adhesion is the limiting factor for the wider application of the technology. Hard coatings, such as chromium nitride (CrN), are commonly used in industry to enhance the tribological and/or corrosion protection of the substrate, and increasingly for decorative applications. The use of interlayers between coating and substrate is well known, i.e., a thin titanium layer between titanium nitride (TiN) coating on 304 stainless steel [1]. This interlayer can improve adhesion by reduction of substrate surface oxide layers and by chemical bonding to the coating. Additionally such layers can provide a buffer for mechanical properties: reducing the 'stress gradient' between the coating and substrate interface; and giving a 'composition gradient' when the coating is very different to the substrate, such as diamond-like carbon (DLC) coating on steel, i.e., Steel / Ti / TiN / TiC / DLC [2].

A recent industrial survey undertaken by NPL [3] reviewed the adhesion test methods used in UK industry and contrasted it to a similar report on US adhesion testing undertaken by NIST [4]. It concluded by stating that although there is a plethora of qualitative test methods for measuring the adhesion strength of coatings, few test methods are quantitative and only a limited number of these are used by industry. The development of international standards for quantitative test methods was considered important by industry both in the UK and internationally, with most interest shown in the development of four-point bend, indentation, scratch, tensile and thermal tests.

Adhesive failure is often a two-stage process. When a coating/substrate system is under sufficient tensile stress it becomes energetically favourable for through-thickness cracks to develop in the coating. Cracks preferentially initiate at coating defects. A through-thickness crack will result in a stress concentration at the corner of the coating adhering to the interface. The crack may therefore propagate along the coating-substrate interface, relieving this stress concentration, propelled by the elastic energy released by the through-thickness cracking event. When meeting they can cause coating spallation. Coating spallation can also be caused through other mechanisms such as buckling and wedge failures [5, 6]. By modifying the effective adhesion of a coating in a controlled and repeatable method the ability of each adhesion test to discriminate between adhesion levels in similar coatings can be studied.

An interlaboratory exercise (ILE) was undertaken to evaluate and compare test methods for adhesion of thin coatings to aid the long-term development of a simple quantitative engineering test for coating adhesion.

2. EXPERIMENTAL.

2.1. SCOPING STUDY.

A scoping study was undertaken at NPL prior to the ILE to test the sample response to different adhesion tests and to aid the writing of a common test proforma to be used by all participants. Adhesion tests undertaken with titanium nitride on AISI 304 stainless steel found that this material combination was unsuitable for an ILE due to the very high adhesion and low fracture toughness of the coating, which made it difficult to observe any delamination unless extreme stresses were applied. To improve the chance of observing adhesive failure a less adherent and/or higher fracture toughness CrN coating was chosen.

Adhesion of CrN was controlled using a thin interlayer. For the scoping study two interlayers were designed to reduce adhesion. An Au/Pd (60:40 wt.%) interlayer was intended to provide a ductile region between coating and substrate and disrupt any chemical bonding between coating and substrate. This was deposited on polished coupons using a small sputter chamber designed to apply conductive coatings for scanning electron microscopy (SEM) specimens. Coating thickness was measured gravimetrically at ~35nm. The second interlayer was an amorphous carbon layer again used to contaminate the interface and reduce chemical and mechanical bonding. The carbon interlayer was deposited using a carbon arc evaporator, similarly designed for SEM work. Several arc pulses were required to get a visible coating. After deposition of the CrN coating on the carbon interlayer large scale delamination of the coating from the substrate was observed. The carbon interlayer had reduced adhesion so much that when cooling from deposition temperature the differential thermal contraction of the coating and substrate was enough to cause the coating to spall (**Figure 1**). The Au/Pd layers did not result in spallation. Rockwell indentation and 4 –point bend testing showed some differences in coating adhesion. Therefore the Au/Pd interlayer was chosen for the ILE coupons and the thickness was varied to obtain different adhesion levels. It was hoped that the ILE test results would allow discrimination between coatings with and without an interlayer and between the different interlayer thicknesses.

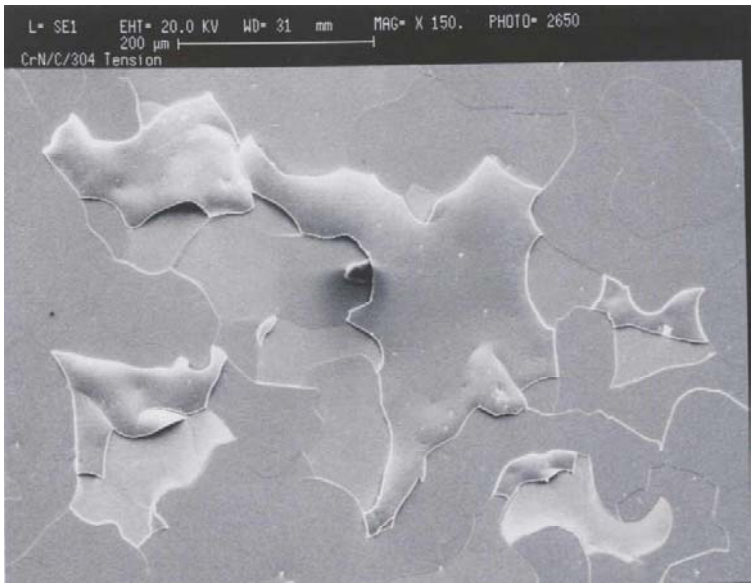

Figure 1. *CrN coating on AISI 304 stainless steel with carbon interlayer. Coating spallation induced by differential thermal expansion coefficients when cooling from deposition temperature.*

2.2. INTERLABORATORY EXERCISE TEST COUPONS.

The substrate material was AISI 304 stainless steel in 3mm thick 'bright sheet' form. Coupons of size 10mm x100mm were spark eroded to minimise work hardening. Each coupon was etched with a unique reference number. A thin surface oxide layer was formed during the spark erosion and was removed with a light abrasive cleaner. Since the sheet was received with a bright finish no subsequent polishing was required. Coupons were ultrasonically cleaned in iso-propanol and hot air dried before coating deposition.

2.2.1 DEPOSITION.

About 400 samples were required for the ILE and so the 'one off' sample preparation route, used in the scoping study, was modified. Twenty-five and fifty nm thick interlayers of Gold-Palladium (60:40 wt. %) were deposited at NPL using electron beam physical vapour deposition (EB-PVD). Thickness was controlled with a piezo-crystal based thin film monitor. Measurements of coating reflectance indicated that the 25nm thick films were not fully dense. The coupons were subsequently coated with CrN to an NPL specification, deposited by reactive EB-PVD at Tecvac Ltd, a UK coatings supplier. A novel cassette was developed by Tecvac to allow a large number of coupons to be coated in one batch (**Figure 2**). A nominal CrN coating thickness of 5µm was applied to three batches of 130 substrates grouped by interlayer type (no interlayer, 25nm interlayer and 50nm interlayer).

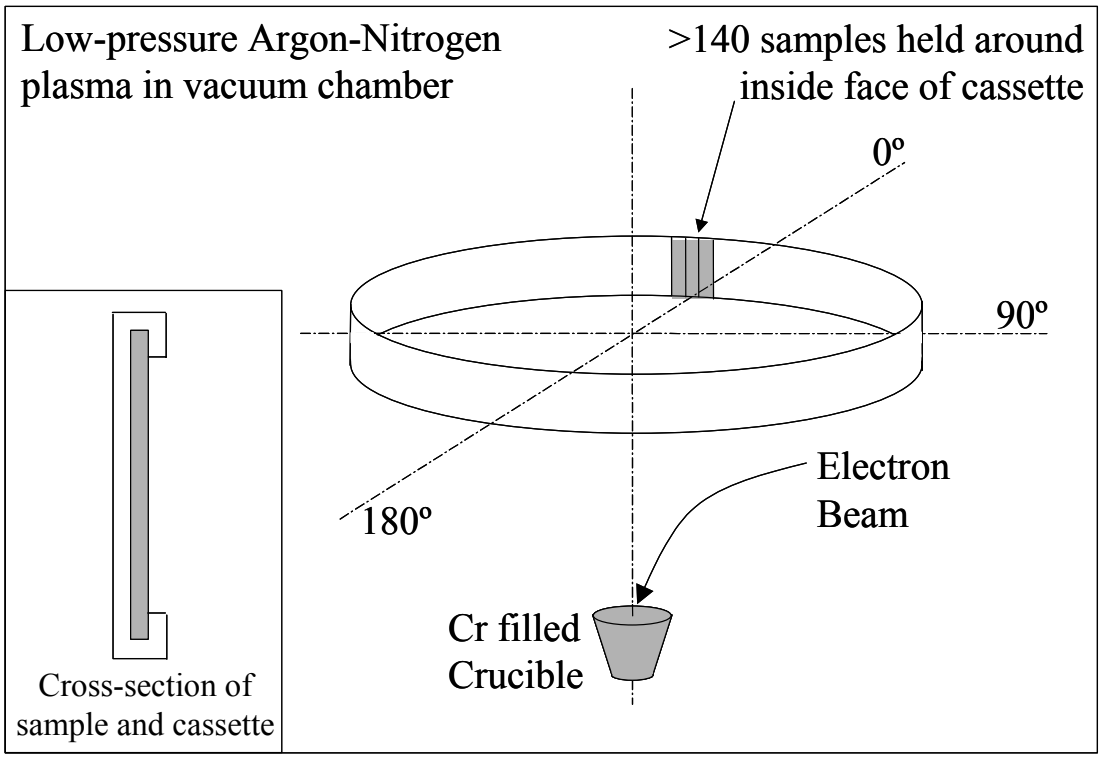

Figure 2. *Schematic of EB-PVD coater. Up to 140 coupons held parallel to coating flux in a novel cassette. Insert shows a cross section of coupon and cassette.*

2.2.2. CHARACTERISATION.

Every tenth coupon was characterised for thickness using a Fischersope X-RAY XDL. This uses the x-ray fluorescence method (XRF), where the secondary x-ray emission intensity of a material is related to thickness when the energy and intensity are calibrated against a known standard [7]. Nine measurements of thickness were taken, equispaced along the coupon. The Fischersope X-RAY XDL was calibrated against a sample with a known thickness of CrN deposited without an interlayer on test coupon. Coating residual stress was determined with a Siemens D500 diffractometer using Cr-Kα radiation set up in Bragg-Bentano geometry. Nanoindentation using an MKS Nanoindenter II with a Berkovich stylus was performed on one coupon from each batch to get nominal values of coating hardness and elastic modulus. Indentations were performed at a range of loads from 5mN to 30mN. Hardness and modulus were plotted against the ratio of contact radius, *a*, to coating thickness, *t*, to allow a depth invariant value to be extrapolated (**Figure 3**). This gives a 'coating only' value unaffected by substrate at $a/t = 0$ [8]. Hardness and modulus data is presented in **Table 1**, standard errors were calculated using the range of possible extrapolations to the intercept.

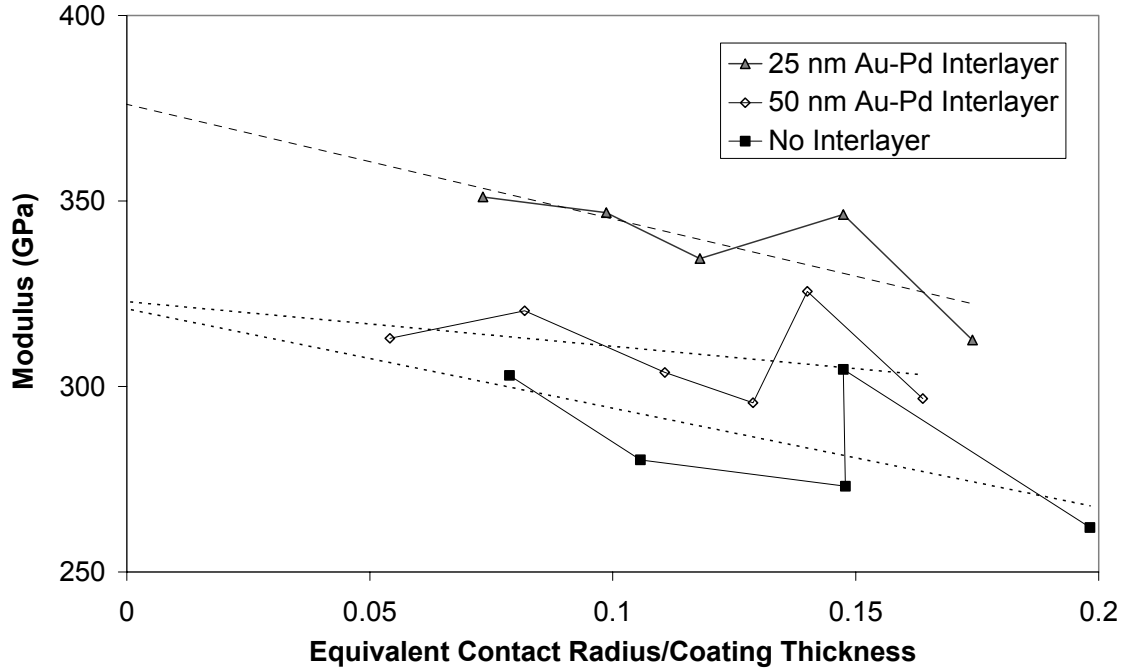

Figure 3. *Extrapolation of nanoindentation data for coating modulus independent of substrate.*

Table 1. *Depth invariant hardness and modulus by nanoindentation of CrN coated AISI 304 stainless steel coupons for each interlayer thickness. Standard errors (1 standard deviation) are quoted.*

Interlayer Thickness	***Hardness (GPa)***	***Modulus (GPa)***
0nm	25 ± 3	321 ± 25
25nm	33 ± 1	376 ± 18
50nm	28 ± 3	323 ± 17

2.3. INTERLABORATORY TESTS.

Detailed test proformas were designed for Rockwell indentation and scratch testing. Some laboratories agreed to perform additional tensile and four-point bend tests. All participants were asked to calibrate equipment traceable to national calibration standards. The newly certified DLC coated steel scratch test reference material [9] was also distributed to confirm calibration of scratch testing equipment. Test conditions are summarised in **Table 2**.

Table 2. *Interlaboratory Test Conditions.*

Test Type	***Test Conditions***		***Mandatory Inspections and Calibrations***
Rockwell Indentation	5 indents per coupon Rockwell 'C' Diamond Stylus (120° cone angle, 200 μm radius) 10 kg pre-load 150 kg total load Spot anvil if available		Stylus inspection for defects (Vertical displacement and Load) or (Standard hardness reference material)
Scratch	5 scratches per coupon Rockwell 'C' Diamond Stylus (120° cone angle, 200 μm radius) 100 N/min loading rate 10 mm/min horizontal displacement rate		Stylus inspection for defects Horizontal displacement Load Stage planarity
	DLC Reference Material 5 N start load 45 N end load	*CrN Coupon* 0 N start load 30 N end load	
Tensile	10 N pre-load 1 mm/min crosshead displacement rate		Vertical displacement Load
Four-Point Bend	20 mm top roller separation 40 mm bottom roller separation 10 N pre-load 1 mm/min crosshead displacement rate		Vertical displacement Load
Thermal (NPL only)	5 ˚C/min heating rate		Temperature

3. RESULTS AND DISCUSSION.

3.1. DEPOSITION AND CHARACTERISATION.

Variations in coating thickness were observed both within coupon, within batch, and between batches. Within the coupon the coating thickness was greater at the bottom of the specimen compared to the top. This was expected as the bottom of the coupon was closer to the EB-PVD crucible (**Figure 2**) and would have received an increased coating flux. Thickness variations with the batches could have been caused by slight mis-alignment of the coupon cassette over the crucible. Residual stress in the coatings followed broadly similar trend to within batch coating thickness (**Figure 4**). CrN thickness varied between batches by about 10%.

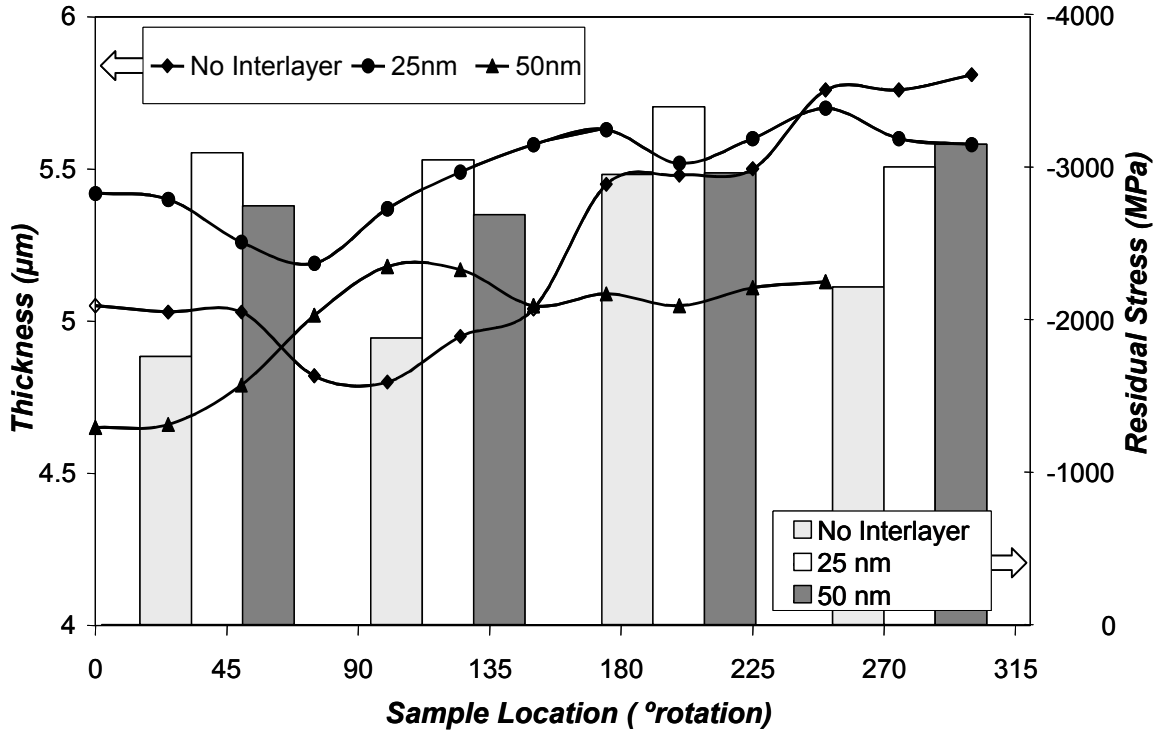

Figure 4. *Average thickness and residual stress for ILE coupons. Thickness (line chart) was measured on every tenth coupon per batch, position shown relative to 0º line on cassette in Figure 2. Residual stress was measured by XRD on four coupons per batch equispaced around the cassette.*

Values for hardness and modulus for each coupon type are given in **Table 1**. One coupon per interlayer thickness was tested. The CrN coated coupon with the 25nm thickness interlayer had an elastic modulus nearly 20% higher than the others, residual stress (**Figure 4**) for this batch was also higher. The reasons for this are not known but this could have resulted from several mechanisms, i.e., a slight variation in process stoichiometry leading to deposition of a CrN analogue, such as a mixture of CrN and Cr_2N.

Despite best efforts there were differences when increasing from laboratory scale to commercial scale production. This led to a significant change in the failure modes observed. This variation shows the absolute necessity of having well defined cleaning, interlayer deposition and coating deposition protocols to produce a standardised coating with uniform adhesion.

3.2. ROCKWELL INDENTATION.

SEM micrographs of indents from the scoping study are shown in **Figure 5**. The $CrN_{NO\ INTERLAYER}$ coupon (**Figure 5a-b**) showed increased Hertzian (ring) cracking around the indent compared to the $CrN_{Au/Pd\ INTERLAYER}$ coupon (**Figure 5c-d**). These cracks had cohesive micro-spallations along the length, similar to those observed with the high load scratch tests. Both coupons showed radial cracks extending out from the indent. With the $CrN_{Au/Pd\ INTERLAYER}$ coupon these induced coating delamination.

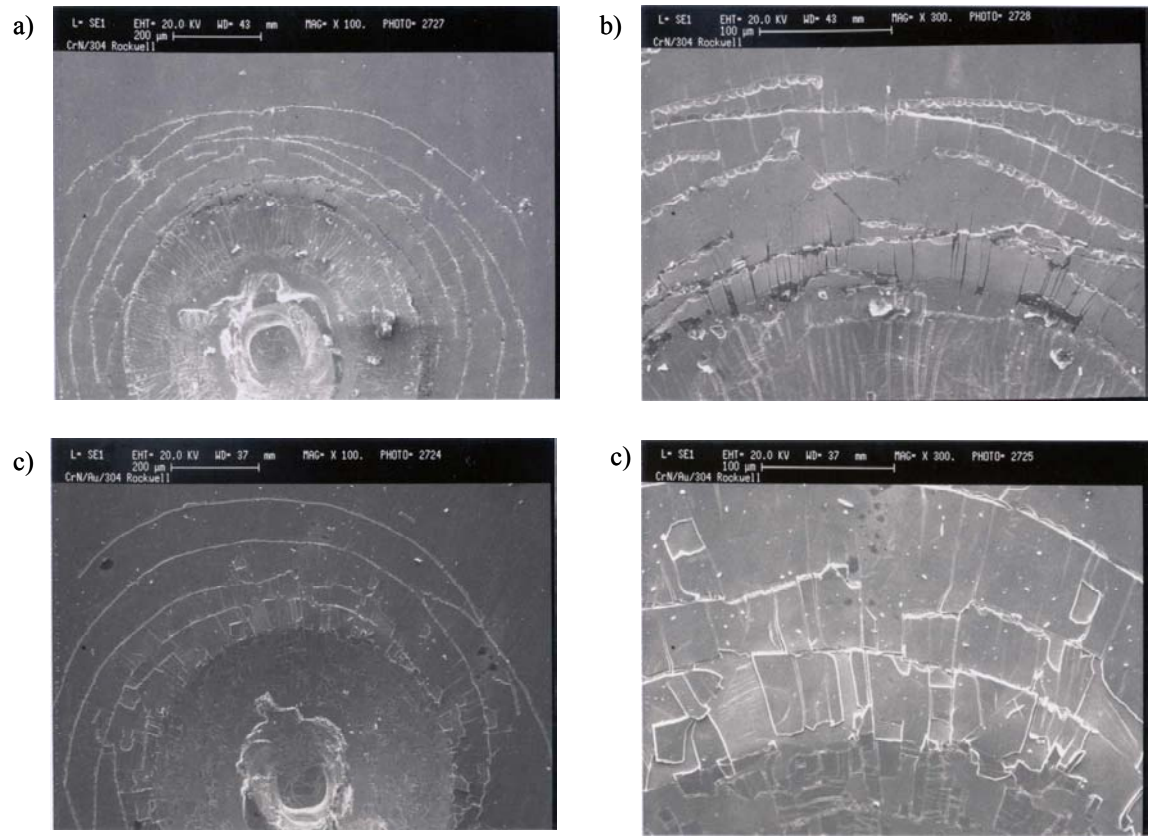

Figure 5. *Scanning electron micrographs of Rockwell indents from the scoping study. a-b) CrN coating, no interlayer; c-d) CrN coating, 35nm gold-palladium interlayer.*

However, in the ILE, Hertzian cracking was present in only one of the eight sets of data returned. No discrimination between interlayers was possible from radial crack spacings. The small changes in sample preparation route between the scoping study and ILE led to a considerable difference in Rockwell indentation response. Indentation diameter of indents taken on the uncoated side of the coupons were used as a calibration check. The values of indent diameter returned indicated that all equipment was properly calibrated (or the test equipment was relatively insensitive to calibration error).

3.3. SCRATCH TESTING.

A detailed failure event description was given to each participant to ensure a standardised method for identification and calculation of L_{C1}, L_{C2} and L_{C3} critical loads. Micrographs of the BCR-692 scratch test reference material failure events were taken from literature [10],

micrographs of the CrN failure events (**Figure 6**) were taken from scratches performed at NPL.

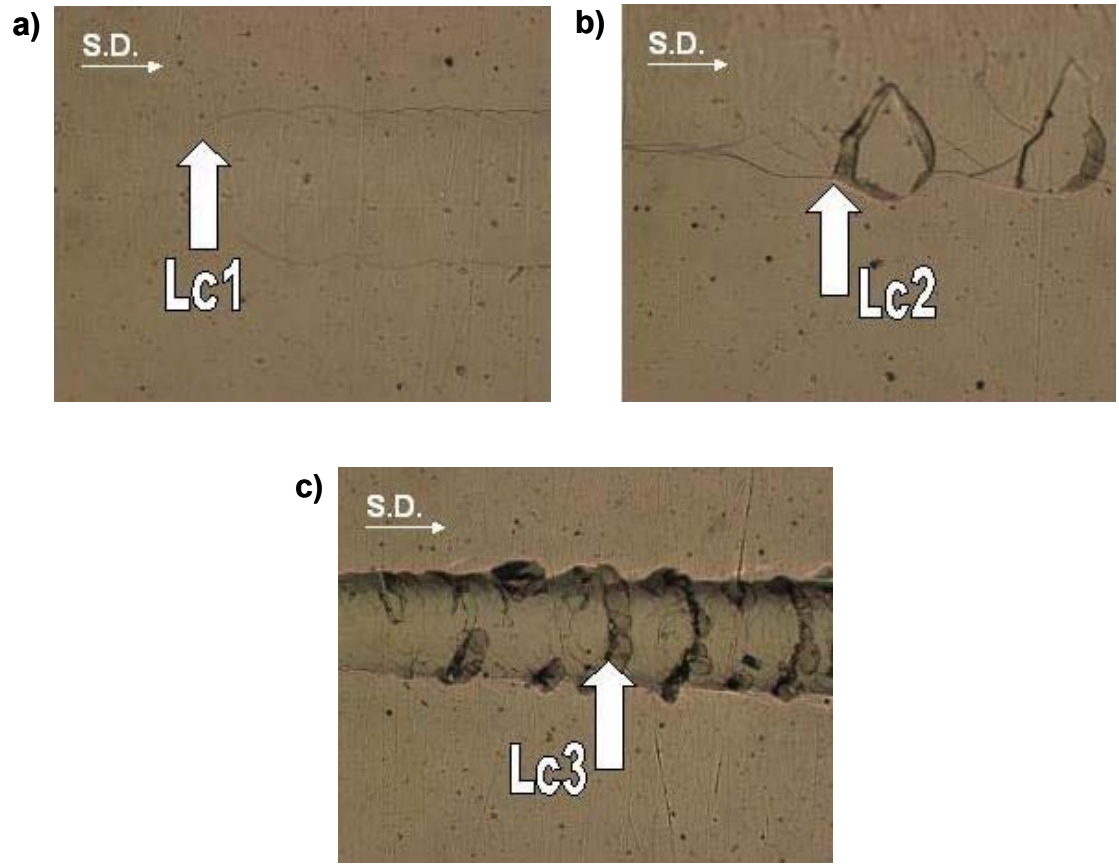

Figure 6. *Micrographs of critical load failure events for the CrN coating. Scratch direction (SD) is from left to right. a) LC1; b) LC2; c) LC3.*

Out of the nine laboratories undertaking scratch testing five submitted data for the DLC reference material (**Figure 7**). This material has well characterised failure mechanisms at certified values of critical load, within upper and lower verification ranges. One laboratory (Lab 7) reported an L_{C1} value ~2% below the lower verification range (**Figure 7a**). As the L_{C2} value returned was similarly low, but just within the verification range, it is likely the stylus was sharper than expected as stylus shape has a greater effect on L_{C1} and L_{C2} values compared to L_{C3} values. Another laboratory (Lab 4) reported an L_{C3} value ~23% below the lower verification range (**Figure 7c**). As this laboratory had a low test standard deviation it was likely that there was either mis-identification of the failure event or some issues with machine stiffness, with the stylus experiencing a stick-slip mechanism at higher loads. All other laboratories reported data within the verification ranges indicating acceptable calibration. Two laboratories who did not submit data for the DLC reference material had the highest and lowest values of critical loads reported for the CrN coupons. This suggests that the equipment was not calibrated or did not conform to the EU scratch testing standard (ENV 1071-3) [11].

Scratch testing of the CrN coating showed a common mode of damage progression for all coupons. As scratch loading increased, forward chevron cracks formed at the side of the

scratch (L_{C1} failure mechanism, **Figure 6a**). When the crack spacing was sufficiently close, cohesive spallation along crack borders occurred (L_{C2} failure mechanism, **Figure 6b**). This was followed by gross interfacial shell shaped spallation (L_{C3} failure mechanism, **Figure 6c**) as the cracks propagated over the scratch width and coating was removed. As load increased further there was an increasing density of conformal type buckling cracks, gross reverse chevron cracks with micro-spallation on the trailing edges, and a discontinuous ductile perforation through the coating.

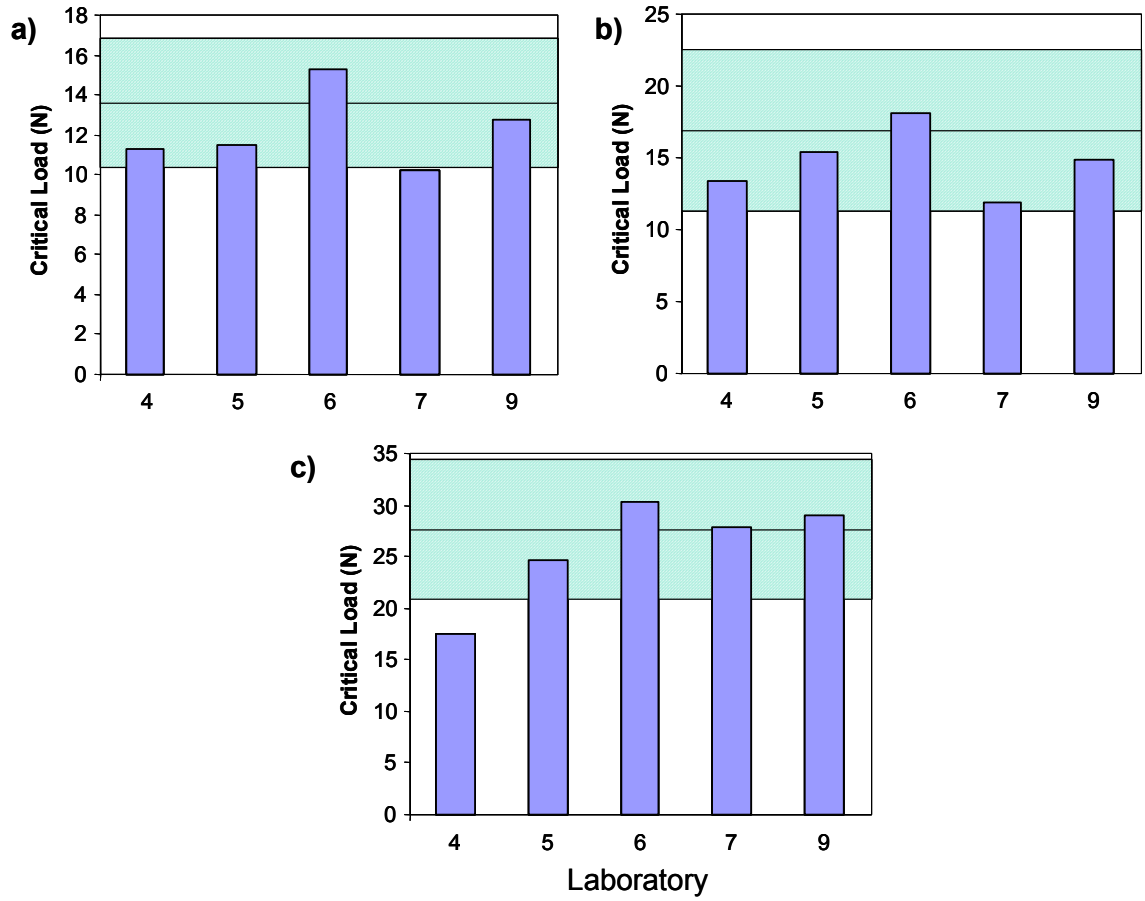

***Figure** 7. ILE critical loads for the BCR-692 diamond-like carbon coated scratch test reference material. Shaded regions indicate upper and lower verification ranges for critical load. a) LC1; b) LC2; c) LC3.*

Scratch testing of CrN was performed over a load range of 0N to 30N. The L_{C1} failure load occurred early in the scratch, typically around 3N. This was sometimes masked by an indent caused when the stylus 'contacted' the surface when attempting to apply a 'zero' load. As this was not machine specific within the ILE it must be concluded that great care must be taken when approaching the surface prior to low load scratching.
There was considerable experimental scatter in the data submitted for the CrN coupons (**Table 3**) and it was not possible to discriminate between interlayer types from values of critical load.

An additional set of 'nano' scratch tests were performed by Lab 10 from 1mN to 1000mN with a loading rate of 1 N/min using a 20µm radius diamond tip. L_{C1}, L_{C2} and L_{C3} failure events were observed for the BCR-692 material. No L_{C3} failure events were observed on the CrN coatings at maximum load and the L_{C2} was difficult to isolate from the large number of brittle events. Whilst there was no direct correlation between the nano and macro critical loads, the nano critical loads were closely grouped with a low standard deviation. Unfortunately the three other laboratories who volunteered to perform nano scratching failed to return data, so no conclusions can be reached on the suitability of the BCR-692 material as a nano scratch reference material or the interlaboratory repeatability of the nano-scratch technique.

Table 3. *Critical loads (L_{C1}, L_{C2} & L_{C3}) of CrN coated AISI 304 stainless steel coupons for each interlayer thickness. * No reference scratch results submitted: unvalidated data.*

Lab	***Interlayer Thickness***	***L_{C1}***		***L_{C2}***		***L_{C3}***	
		Ave (N)	***Std Dev***	***Ave (N)***	***Std Dev***	***Ave (N)***	***Std Dev***
1*	0 nm	2.32	0.33	4.11	0.83	12.85	1.52
	25 nm	3.52	0.60	5.70	0.69	13.14	2.32
	50 nm	2.28	0.25	6.61	0.57	10.94	1.39
2*	0 nm	2.13	0.68	6.59	0.78	10.25	0.90
	25 nm	4.24	0.57	5.22	0.89	8.92	1.13
	50 nm	2.73	0.30	6.25	0.69	10.39	0.96
3*	0 nm	9.43	0.14	10.23	0.14	14.38	0.89
	25 nm	9.85	0.42	10.63	0.60	15.82	1.58
	50 nm	9.24	0.54	10.11	0.60	14.54	1.32
4	0 nm	1.38	0.16	5.14	0.22	10.18	0.84
	25 nm	2.00	0.20	5.44	1.34	9.50	0.97
5	0 nm	3.85	3.96	6.05	0.24	11.26	1.07
	25 nm	4.21	0.67	6.49	0.37	10.95	12.14
	50 nm	2.43	0.34	6.66	0.77	12.14	0.89
6	0 nm	2.06	0.15	5.36	0.45	11.78	1.13
	25 nm	3.80	0.31	5.32	0.45	10.30	0.76
	50 nm	2.54	0.43	6.40	0.58	10.96	0.67
7	0 nm	2.80	0.20	6.78	0.72	12.24	0.68
	25 nm	2.91	0.17	7.27	0.60	12.49	0.84
	50 nm	2.41	0.19	7.17	0.53	12.48	0.47
8*	0 nm	1.21	0.28	2.12	0.56	7.57	2.82
	25 nm	0.75	0.36	1.67	0.69	4.87	2.57
	50 nm	0.85	0.41	2.30	1.15	8.87	2.97
9	0 nm	3.18	0.25	7.38	0.31	10.99	0.53
	25 nm	3.34	0.27	6.45	0.50	9.38	0.33
	50 nm	2.97	0.08	7.14	0.42	10.81	0.60

3.4. TENSILE AND FOUR-POINT BEND TESTING.

Tensile and four-point bend tests were undertaken at two laboratories as an extension to the main ILE. Test conditions are shown in **Table 2**. No coating spallation was observed at the maximum strain (7%) by either laboratory so adhesion values could not be calculated. The expected coating failure mechanism was through-thickness cracking followed be spallation of the coating as cracks propagated along the coating-substrate interface. However, micrographs taken throughout the tensile test by Lab 1 showed a different mechanism: delamination along the interface followed by through-thickness cracking (**Fig. 8**). Onset of coating failure was detected by acoustic emission (Lab 1) and by iterative testing (Lab 2). The iterative test method involved performing several tests on fresh samples, increasing the maximum strain for each test and looking for evidence of fracture optically. It was expected that the values of strain at first fracture for the nominally similar CrN coatings would be close for both interlayer thickness and test type. Trends of first-fracture strain vs. interlayer thickness were opposite between labs, as shown in **Table 4**. During both tensile and four-point bend tests the acoustic emission trace remained at a low background level until a sharp rise, attributed to fracture events, was detected. First-fracture strain was calculated from this point. Laboratory 2 recorded self-consistent strains, whereas laboratory 1 did not, suggesting that the iterative test method was better at detecting the first-fracture event than acoustic emission.

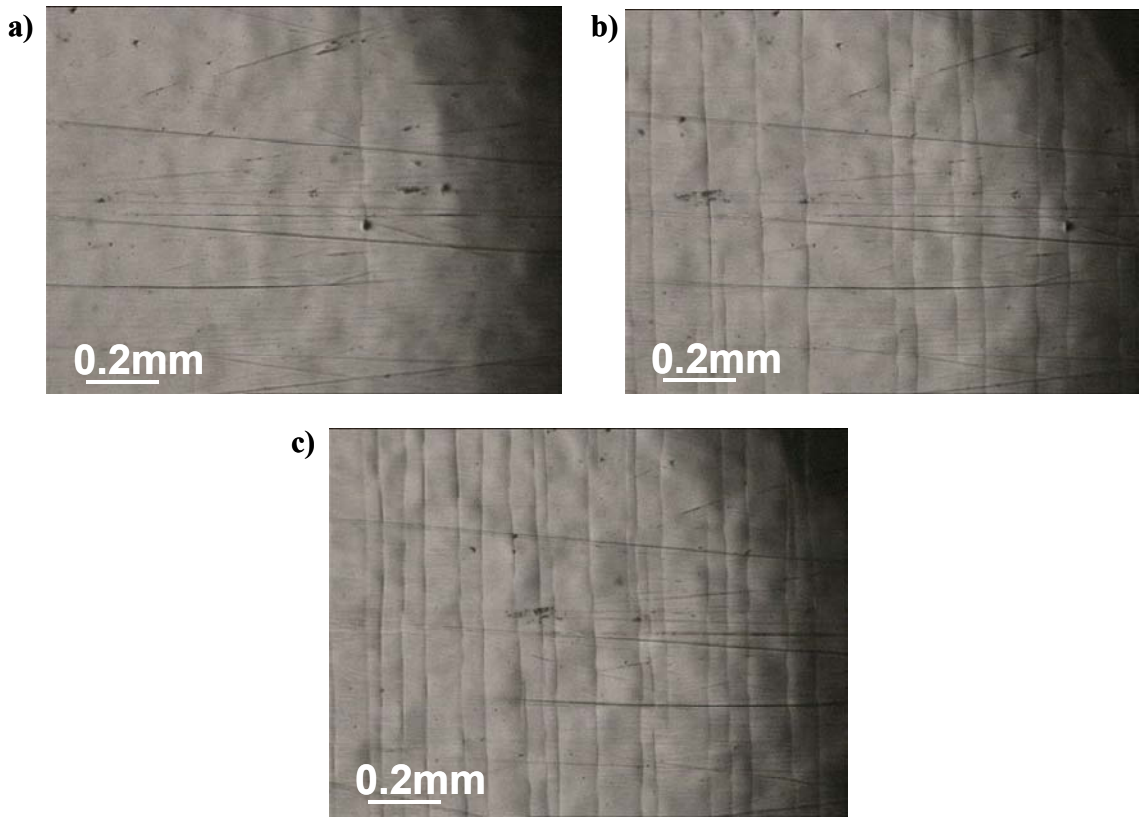

Figure 8. *Fracture micrographs from tensile test for CrN coated steel with no interlayer. a) 0.65% strain; b) 0.84% strain; c) 1.10% strain. Loading axis was horizontal relative to micrograph. Delamination between substrate and coating is observed before cracking.*

Table 4. *Strain at first fracture event in tensile and four-point bend tests of CrN coated AISI 304 stainless steel coupons for each interlayer thickness.*

Test	***Laboratory***	***Average Fracture Strain (%)***		
		No Interlayer	***25nm Interlayer***	***50nm Interlayer***
Tensile	1	0.62	0.87	1.07
	2	1.15	1.10	1.00
4-point bend	1	0.72	0.54	0.85
	2	1.13	1.24	1.13

3.5. THERMAL TESTING.

Various models have been developed at NPL to predict the response of coated systems under stress [12, 13, 14]. A thermal test was performed at NPL on a 5µm CrN coated coupon (no interlayer) to predict the coating fracture energy under elastic stress. The mismatch in thermal expansion coefficients between coating and substrate was exploited to induce tensile stresses in the coating. The coupon was heated in a furnace at 5ºC per minute. Cracking was first detected by acoustic emission at 500ºC when it became energetically favourable for through-thickness cracks to form and relieve the stress. This failure was analysed using an energy balance technique. The fracture energy for through-thickness cracking is estimated to be 7.66 J/m^2, this corresponds to values for relatively brittle materials [12].

Stress transfer models for ply cracking in composite laminates have been modified by NPL so that they can be applied to the prediction of through-thickness cracking in hard coatings under tensile and bending stresses [13]. An accurate stress analysis (confirmed by comparison of predictions with FEA and boundary element solutions) was used in conjunction with energy balance methods to predict the progressive formation of coating cracks with increasing load. The model also takes into account thermally induced residual stresses (**Table 5**). The model shows close agreement to the experimental data.

Table 5. *Model predictions for stress at first fracture event in tensile and four-point bend tests of CrN coated AISI 304 stainless steel.*

Fracture Stress Mode	***Fracture Stress, Modelled***	***Fracture Stress, Experimental***
Tensile	0.347 GPa	0.324 GPa
Bending Moment/Area	0.250 MN/m	0.257 MN/m

4. CONCLUSIONS.

The thickness variation inherent from the deposition geometry complicated analysis of the results obtained and may have masked small variations in adhesion. It would have been preferable to have coupons held perpendicular to the coating flux instead of parallel, although this would have led to a reduction in batch size and possible increased variations between samples. However, the following conclusions from this study can be made:

- Discrimination between coupons with different interlayers, and therefore adhesion states, was not possible in this study.
- Subtle differences in preparation between scoping study coupons and ILE coupons resulted in a large change in adhesion response.
- Fracture energy, tensile fracture stress and bending moment at fracture stress have been modelled and show good agreement with experimental results.
- The DLC scratch test reference material was tested in a first ‘industrial’ usage. This

reference material was capable of checking equipment calibration and error finding.

5. REFERENCES.

[1] BULL, S. & CHALKER, P., Institute of Materials, Vol. 5, 1992. pp. 205.

[2] VOEVODIN, A., REBHOLZ, C. & MATTHEWS, A., Tribology Transactions, 38, 1995. pp. 829

[3] MAXWELL, A.S., NPL REPORT MATC (A) 49, 'Review of Test Methods for Coating Adhesion', National Physical Laboratory, U.K., 2001

[4] SMITH, D.T., Unpublished research, NIST, 2001.

[5] MENEVE, J., HAVERMANS, D., VON STEBUT, J., JENNETT, N.M., BANKS, J., SAUNDERS, S.R.J., CAMINO, D., TEER, D.G., ANDERSSON, P. & VARJUS, S., Proc World Tribology Congress, 8-12 Sept 1997, Mechanical Engineering Publications Ltd, London, 1997, p.485.

[6] BULL, S., in 'Advances in Surface Engineering Vol. 1 Fundamentals of Coatings', Eds. PK Datta & JS Burnell-Gray, Royal Society of Chemistry Special Publication no 206, 1997, pp. 274.

[7] EN ISO 3497: 2000. Metallic coatings - Measurement of coating thickness - X-ray spectrometric methods.

[8] ISO/CD 14577-4, Metallic materials - Instrumented indentation test for hardness and materials parameters - Part 4: Test method.

[9] European Commission, Community Bureau of Reference, Certified Reference Material, BCR-692, Diamond-like carbon coated steel for scratch testing.

[10] NPL Measurement Good Practice Guide No. 54 The Scratch Test: Calibration, Validification and the use of a certified Reference Material. National Physical Laboratory, U.K., 2003.

[11] EN 1071-3: 2001. Advanced technical ceramics – Methods of test for ceramic coatings – Part 3: Determination of adhesion by a scratch test.

[12] ROBERTS, S.J., McCARTNEY, L.N., & WRIGHT, L.,"Predicting Steady State Interface Debonding in a Two-layer Coated System Under Biaxial Loading and Bending", NPL Report MATC(A)143 (2003).

[13] ROBERTS, S.J. & McCARTNEY, L.N., "Predicting Steady State Interface Debonding in a Multi-layered Coated System Under Biaxial Mechanical and Thermal Loading", NPL Report MATC(A)144 (2003).

[14] ROBERTS, S.J. & McCARTNEY, L.N., "New Method of Measuring Elastic Properties of Coatings: Part I – Theoretical Approach", NPL Report MATC(A)146 (2003).

ACKNOWLEDGMENTS.

This project was undertaken with funding from Department of Trade and Industry, UK, under the 'Characterisation and Performance of Materials' programme. Tony Fry and Tony Maxwell performed the XRD and nanoindentation at NPL. Most thanks are due to the interlaboratory participants for providing the data in this paper.

ANNEXE Independent evaluation of toughness: Interface and film

Hideaki Nagasawa
Department of Machine Intelligence and Systems Engineering,
Graduate School of Engineering, Tohoku University, Japan.

In order to evaluate the toughness of interface and the toughness of films, samples were processed into two kinds of specimen configurations. These are schematically illustrated in **Figure A1**, and here we call them as "film brick" and "film projection", respectively. The interface toughness was measured using film bricks, while film projections were used to evaluate the film toughness. The film brick was loaded horizontally by a diamond needle. At a certain load level, the film brick was pushed off away, when the crack ran unstably along the interface. Toughness of interface was estimated by referring the experimental result to the simulation of crack extension with assumed values of toughness. In the film projection, a notch was set parallel to the edge of projection. Transverse load was applied at the intersection of projection edge and the perpendicular bisector of the notch. The crack extended unstably from the notch tip, and the toughness was calculated with the load at the point of unstable fracture.

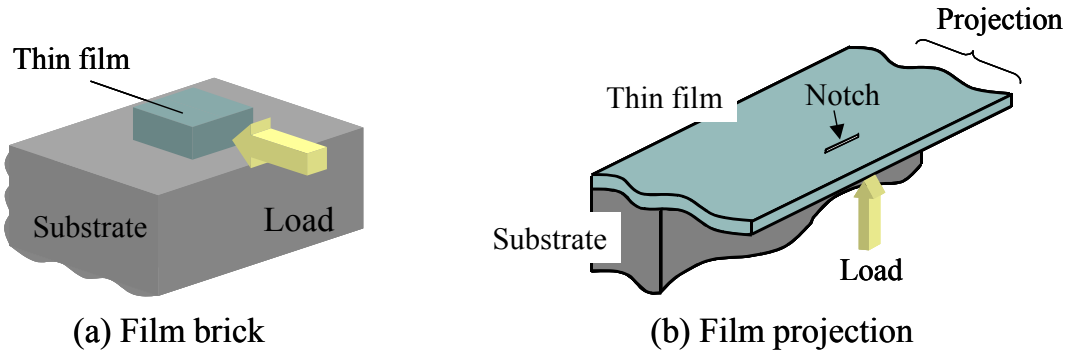

Figure A1. *Two specimen configurations*

Table A1 shows the data averaged over a number of specimens (bricks or projections) for each sample. The above-mentioned simulation needs Young's modulus of the film and the residual stress in the film, which were obtained as also presented in **Table 1** by applying the technique [A1]. The difference in the levels of adhesion is clearly seen between the samples with and without interlayers, while no significant effect of interlayers is observed in the toughness of films. The difference in adhesion might not be evaluated by conventional techniques, e.g. scratch test, because the toughness of interface is much larger than the toughness of film for the case without the interlayer.

Table A1. *Toughness and other mechanical properties of CrN on AISI 304*

Interlayer (nm)	***Adhesion (J/m2)***	***Cohesion (J/m2)***	***Young's modulus (GPa)***	***Residual strain (%)***
0	112	40	187	0.83
25	55	54	170	1.12
50	43	39	280	0.66

[A1] S.Kamiya, H.Kimura, K.Yamanobe, M.Saka, H.Abé, Thin Solid Films, **414** (2002) 91-98.